Proc. Inst. Electrostat. Jpn.

静電気学会誌, 21, 2 (1997) 62-68

論　　文

Electrostatic Suspension of 8-inch Silicon Wafer

Jong-Up JEON,* Ju JIN* and Toshiro HIGUCHI*,**

(Received July 3, 1996)

In the field of semiconductor manufacture, there has been a strong demand for contactless wafer handling devices that can manipulate a silicon wafer without contaminating or damaging it. To fulfil this requirement, an electrostatic suspension system for an 8-inch silicon wafer is proposed. Since electrostatic suspension systems without any active control of electrostatic forces are inherently unstable, the electrostatic forces acting on the wafer are actively controlled on the basis of the position/attitude of the wafer. This paper describes the design considerations for the electrostatic wafer suspension system, the dynamic model, stabilizing feedback controller and experimental system configuration. Experimental results show that an 8-inch silicon wafer can be stably levitated at a gap length of 0.3 mm by employing voltages of approximately ±0.5 kV. The lateral dynamic characteristics and wafer potential are also measured and presented.

1. Introduction

In wafer handling devices utilized in ultra-high vacuum and clean-room environment, it is essential to avoid particle generation that arises from mechanical interaction between silicon wafers and the handling tools. At present, industrial wafer handling equipment used in ultra-high vacuum and clean-room environment is mainly centered around robotic manipulators that handle the wafer through direct mechanical contact. Therefore, there is a necessity to develop contactless and friction-free wafer manipulation systems. Several wafer handling devices based on electromagnetic suspension have already been developed.[1-3] However, in these systems the wafer is placed directly on a magnetically levitated carrier since electromagnetic forces can not exert forces on non-ferromagnetic materials such as silicon wafers, which results in direct mechanical contact. Furthermore, air and acoustic levitation techniques have also been developed.[4,5] It is apparent that these techniques are not appropriate in a vacuum environment.

Electrostatic suspension has the potential to realize contactless support of the wafer. Compared to electromagnetic levitation, electrostatic suspension has several advantages. Firstly, electrostatic suspension can suspend various materials such as conductive materials, semiconductors and dielectric materials, in contrast to electromagnetic levitation which can levitate only ferromagnetic materials. Secondly, the geometries of stator electrodes which are used as actuators are typically planar structures and easy to manufacture in contrast to the 3-dimensional structures of electromagnetic circuits. Thirdly, electrostatic suspension generates less heat than electromagnetic levitation. In electrostatic suspension, only submicroampere-order current flows through the electrodes and the suspended object, and thus heat generation can be neglected. This means that electrostatic suspension may be more suitable for use in vacuum environments.

Despite the before mentioned advantages, electrostatic suspension has not been employed in industry except for such special applications as electric vacuum gyros[6] since the maximum attainable electrostatic force itself is weak.[7] In this paper, we will show that electrostatic suspension has the ability to provide sufficient suspension forces in practical applications. Objects having large surfacial areas, such as disks, are relevant to be suspended. The authors have already succeeded in suspending a 4-inch silicon wafer and a 3.5-inch aluminum disk.[8,9]

In this paper, 8-inch silicon wafers are used as levitated objects. The wafer dynamic model together with stabilizing controller are studied in detail based on the conditions that each degree of freedom is decoupled and the wafer potential is zero. For the stabilizing controller, a decentralized control scheme is used which is practically easier to implement than a centralized control scheme.[9] The lateral wafer dynamic characteristics are investigated experimentally. The wafer potential during suspension is also proven both analytically and experimentally to be near to zero volt.

Keywords: electrostatic suspension, electrostatic force, silicon wafer

* Kanagawa Academy of Science and Technology, East Block 405, KSP, 3-2-1 Sakado, Takatsu-ku, Kawasaki 213, Japan

** Department of Precision Machinery Engineering, The University of Tokyo, 7-3-1 Hongo, Bunkyo-ku, Tokyo 113, Japan

2. Electrostatic Wafer Suspension

2.1 Applicable Electrostatic Force

The attainable maximum electrostatic force is limited by the breakdown of the electric field which arises when the electric field strength becomes greater than a maximum value dictated by the insulating material in the gap. This maximum force yields an upper limit for the mass that can be suspended.

The energy density w contained in the gap, which also represents the electrostatic force per unit surfacial area, is given by

$$w=\frac{1}{2}\varepsilon E^2 \tag{1}$$

where ε and E denote the permittivity and electric field strength in the gap, respectively. In atmospheric environment, the breakdown field strength is approximately 3 kV/mm and results in a maximum force density of 40 N/m^2. In case of wafers having a thickness of 0.725 mm and a mass density of 2.25 g/cm^3 which are used in our experiments, the weight of the wafer per unit surfacial area becomes 16 N/m^2. This indicates that the wafer can be suspended electrostatically without the breakdown of the electric field. In ultra-high vacuum environment, the breakdown electric field strength shows a drastic increase. A sustained electric field strength of 15 kV/mm has been reported at a gap length of 0.254 mm.[6] Therefore, in ultra-high vacuum environments, greater electrostatic forces are applicable for electrostatic suspension.

2.2 Wafer Potential and Particle Contamination

In an electrostatic wafer suspension system, if the wafer potential is high, structural damage of the integrated circuit (IC) elements, in particular, the insulating layer, can occur.[10] This potential also generates electric fields toward the ground and thus will attract particles toward the wafer which can be a source for the failure of the IC elements on the wafer. Therefore, the wafer potential should be kept near zero volt. In our experimental system, this can be achieved through an anti-symmetric distribution of the polarities of the voltages supplied to the electrodes, which will be verified analytically and experimentally.

Another point to be considered in wafer suspension systems is concerned with the strong electric field between the electrodes and the wafer. This electric field is generated even though the wafer potential is zero. Owing to this strong electric field, particles will be accumulated on the wafer. However, it should be noted that in an electrostatic wafer suspension system the overlapping area between the electrodes and the wafer is typically large enough compared to the gap. This means that, apart from the fringe fields at the edges, the electric field is almost confined to the gap region. Therefore, by orienting the working surface of the wafer away from the suspension electrodes, particle accumulation on the working surface can be alleviated.

On the other hand, the fringe field near the edge could attract particles toward the edge of the wafer. However, this may not form a problem considering the fact that in the manufacturing process for highly-integrated semiconductor devices, not the peripheral part but the central part of wafer is used to make IC devices. Another approach is to reduce the fringe fields by forming a guard electrode around the wafer, which is a technique often used in capacitive sensors. In industrial wafer handling equipment, so called electrostatic wafer chucks are being used. These chucks use electrostatic forces to clamp wafers on a flat surface. However, despite the existence of fringe fields, the electrostatic wafer chucks do not possess any additional protection mechanisms to avoid particle attraction toward the edges. This shows that the fringe fields do not form a major problem in practice.

3. Dynamic Model

To implement a stable wafer suspension, it is necessary to control its movement in five degrees of freedom: movements in horizontal plane, vertical movement, pitching and rolling. Among them, the movements in the horizontal plane of the wafer are stabilized without any active control through a restriction force that originates from a relative lateral translation of the wafer with respect to the stator electrode. The wafer movements in the remaining three degrees of freedom are stabilized by actively controlling the attractive forces exerted by the stator electrodes on the wafer.

Figure 1 shows the structure of a stator electrode and the definition of the coordinate system and the terminology. The stator electrode is divided into four sections of which each section acts as an actuator. The four electrodes, which are equally distributed on a plane, have the

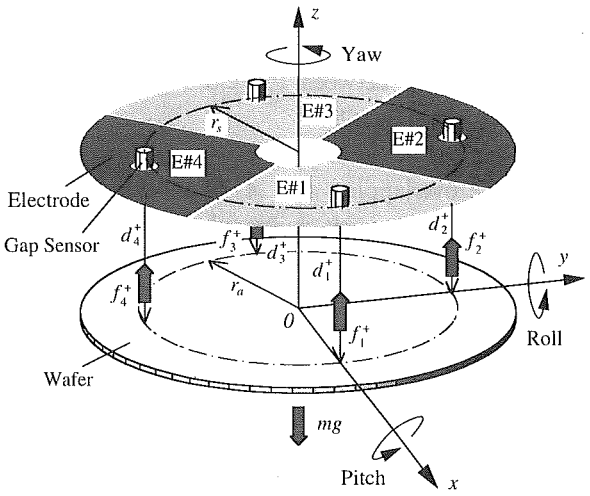

Fig. 1 Structure of stator electrode and definition of coordinate system and terminology.

same geometrical shape and area. To measure the gap length between each electrode and the wafer, a contactless gap sensor is mounted on each individual electrode.

3.1 Nonlinear Equation of Motion

In the following analysis, concerning the linearized variables around the nominal operating points, the superscript "+" denotes the total value, and the subscript "0" denotes the value at the equilibrium state. Symbols without superscript "+" and subscript "0" are small variable terms from the equilibrium state.

We define a reference coordinate frame $\sum(O\text{-}xyz)$ such that when the center line of the wafer coincides with that of the electrodes, the origin O is located at the wafer's center of mass and the z axis is coincident with the center line of the wafer. Each of the distributed forces generated by the electrodes can be treated as an equivalent concentrated force with its point of application at the geometrical center of the electrode.

As mentioned previously, three of the five degrees of freedom of the wafer are actively controlled. Thus we focus the model on these three degrees of freedom.

Let $\boldsymbol{r}^+=(z^+,\ \theta^+,\ \psi^+)^{\mathrm{T}}$, $\boldsymbol{M}=\mathrm{diag}(m,\ J_r,\ J_r)$, $\boldsymbol{f}^+=(f_1^+,\ f_2^+,\ f_3^+,\ f_4^+)^{\mathrm{T}}$, $\boldsymbol{f}_e^+=(f_{ez}^+,\ f_{e\theta}^+,\ f_{e\psi}^+)^{\mathrm{T}}$, where m is the mass of the wafer, J_r is its moment of inertia, z^+ is the z-coordinate of the wafer's center of mass, $(\theta^+,\ \psi^+)$ are the angular displacements of the wafer's rotational axis about the x- and y-axis respectively, f_1^+, f_2^+, f_3^+, f_4^+ are the electrostatic forces produced by the electrodes, and f_{ez}^+, $f_{e\theta}^+$, $f_{e\psi}^+$ are the external forces including the weight of the wafer. Assuming that the wafer is a rigid floating body and its movement is very small, the fundamental equations of motion for the three degrees-of-freedom are described as follows

$$\ddot{\boldsymbol{r}}^+=\boldsymbol{M}^{-1}\boldsymbol{T}_a\boldsymbol{f}^+ +\boldsymbol{M}^{-1}\boldsymbol{f}_e^+ \tag{2}$$

where $\boldsymbol{T}_a$ is the location matrix of the electrodes and is given by

$$\boldsymbol{T}_a=\begin{bmatrix} 1 & 1 & 1 & 1 \\ 0 & r_a & 0 & -r_a \\ -r_a & 0 & r_a & 0 \end{bmatrix} \tag{3}$$

r_a is the distance between the electrode's geometrical center and the origin O.

3.2 Electrostatic Force

When the overlapping area A_j of an electrode j and the wafer is large enough compared with the gap length d_j^+, the capacitance C_j^+ can be approximated as

$$C_j^+=\frac{\varepsilon A_j}{d_j^+},\quad j=1,\ 2,\ 3,\ 4 \tag{4}$$

and the electrostatic force f_j^+ can be expressed in terms of the gap length d_j^+, the voltage V_{aj}^+ supplied to the j'th electrode, and the wafer potential V_f^+

$$f_j^+=\frac{\varepsilon A_j}{2}\left[\frac{V_{aj}^+-V_f^+}{d_j^+}\right]^2,\quad j=1,\ 2,\ 3,\ 4 \tag{5}$$

where ε denotes the permittivity. The above equation shows that V_f^+ should be known in order to compute f_j^+. Figure 2 shows a diagram which represents an equivalent circuit of the electrodes-wafer configuration. In this analysis, the wafer is assumed to be conductive and only the capacitances C_j^+ are considered as impedance elements. Using Kirchhof's law, the wafer potential V_f^+ can be derived as

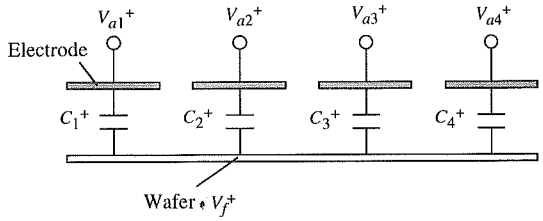

Fig. 2 Equivalent circuit of stator electrodes-wafer configuration.

$$V_f^+=\frac{\sum_{j=1}^{4}(C_j^+V_{aj}^+)}{\sum_{j=1}^{4}C_j^+} \tag{6}$$

During suspension, V_f^+ should be kept to zero, as mentioned before. From (6), the necessary condition for V_f^+ to become zero is

$$\sum_{j=1}^{4}(C_j^+V_{aj}^+)=0 \tag{7}$$

In the following analysis, the wafer potential is assumed to be zero because the voltage of each electrode will be controlled to satisfy condition (7), which will be described in the subsequent section.

3.3 Linearized Equation of Motion

The nonlinear equation of motion (2) is linearized around the nominal operating points under the assumption that the deviations from the nominal values are very small. If we linearize the electrostatic forces (5), then we can write

$$f_j^+=f_{0j}+f_j,\ V_{aj}^+=V_{a0j}+V_{aj},\ d_j^+=d_{0j}+d_j,\quad j=1,\ 2,\ 3,\ 4$$

where $f_{0j}=\frac{\varepsilon A_j}{2}\left(\frac{V_{a0j}}{d_{0j}}\right)^2$, $f_j=k_{Vj}V_{aj}-k_{sj}d_j$ (8)

and k_{sj} and k_{Vj} are the linearization constants which are given by

$$k_{sj}=\frac{\varepsilon A_jV_{a0j}^2}{d_{0j}^3},\ k_{Vj}=\frac{\varepsilon A_jV_{a0j}}{d_{0j}^2} \tag{9}$$

Let $\boldsymbol{r}_0=(z_0,\ \theta_0,\ \psi_0)^{\mathrm{T}}$, $\boldsymbol{r}=(z,\ \theta,\ \psi)^{\mathrm{T}}$, $\boldsymbol{f}_0=(f_{0j})^{\mathrm{T}}$, $\boldsymbol{f}=(f_j)^{\mathrm{T}}$, $\boldsymbol{f}_{e0}=(f_{e0z},\ f_{e0\theta},\ f_{e0\psi})^{\mathrm{T}}$, $\boldsymbol{f}_e=(f_{ez},\ f_{e\theta},\ f_{e\psi})^{\mathrm{T}}$, $\boldsymbol{d}=(d_j)^{\mathrm{T}}$, $\boldsymbol{V}_a=(V_{aj})^{\mathrm{T}}$, $\boldsymbol{K}_s=\mathrm{diag}(k_{sj})$, $\boldsymbol{K}_V=\mathrm{diag}(k_{Vj})$, where $j=1,\ldots,4$. By defining $\boldsymbol{r}^+=\boldsymbol{r}_0+\boldsymbol{r}$, $\boldsymbol{f}^+=\boldsymbol{f}_0+\boldsymbol{f}$ and $\boldsymbol{f}_e^+=\boldsymbol{f}_{e0}+\boldsymbol{f}_e$ and using (8), the equation of motion (2) can be rewritten as

$$\ddot{\boldsymbol{r}}=\boldsymbol{M}^{-1}\boldsymbol{T}_a\boldsymbol{f}_0+\boldsymbol{M}^{-1}\boldsymbol{f}_{e0}-\boldsymbol{M}^{-1}\boldsymbol{T}_a\boldsymbol{K}_s\boldsymbol{d}+\boldsymbol{M}^{-1}\boldsymbol{T}_a\boldsymbol{K}_V\boldsymbol{V}_a+\boldsymbol{M}^{-1}\boldsymbol{f}_e\quad(\ddot{\boldsymbol{r}}_0=\boldsymbol{0}) \tag{10}$$

Let $\boldsymbol{V}_{a0}$ be the bias voltage which is defined by $\boldsymbol{V}_{a0}=(V_{a0j})^{\mathrm{T}}$, where $j=1,\ldots,4$. Then $\boldsymbol{V}_{a0}$ can be determined from (7) and (10). At the equilibrium state, $\boldsymbol{V}_{a0}$ satisfies

the following steady-state equation

$$\boldsymbol{M}^{-1}\boldsymbol{T}_a\boldsymbol{f}_0+\boldsymbol{M}^{-1}\boldsymbol{f}_{e0}=\boldsymbol{0} \tag{11}$$

In addition, referring to (7), the condition for zero wafer potential at the equilibrium state is

$$\boldsymbol{C}_0^{\mathrm{T}}\boldsymbol{V}_{a0}=\boldsymbol{0} \tag{12}$$

where $\boldsymbol{C}_0=(C_{0j})^{\mathrm{T}}$; $C_{0j}=(\varepsilon A_j)/d_{0j}$, $j=1,\ldots,4$. $\boldsymbol{V}_{a0}$ is selected such that (11) and (12) are satisfied. Note that there is redundancy in solving (11) and (12) to obtain $\boldsymbol{V}_{a0}$. When determining a solution, the minimization of the variance of the absolute values of the electric field strengths in each gap can be applied as a criterion. Considering the weight of the wafer as the only external force and assuming that $A_j=A$, where $j=1,\ldots,4$, we obtain six feasible solutions having zero variance. From these solutions, we select the following one

$$V_{a01}=d_{01}E_0,\ V_{a02}=-d_{02}E_0,$$
$$V_{a03}=d_{03}E_0,\ V_{a04}=-d_{04}E_0 \tag{13}$$

where E_0 is the electric field strength at the equilibrium state and is given by

$$E_0=\left(\frac{mg}{2\varepsilon A}\right)^{1/2} \tag{14}$$

In the following analysis, it is assumed that a positive voltage is applied to electrodes #1 and #3, and a negative voltage to electrodes #2 and #4, which ensures a zero wafer potential (for a proof, see appendix).

Next, consider the following geometric relation between $\boldsymbol{r}$ and $\boldsymbol{d}$

$$\boldsymbol{d}=-\boldsymbol{T}_a^{\mathrm{T}}\boldsymbol{r} \tag{15}$$

Using (10), (11) and (15), the linearized dynamic equation of motion of the wafer becomes

$$\ddot{\boldsymbol{r}}=\boldsymbol{M}^{-1}\boldsymbol{T}_a\boldsymbol{K}_s\boldsymbol{T}_a^{\mathrm{T}}\boldsymbol{r}+\boldsymbol{M}^{-1}\boldsymbol{T}_a\boldsymbol{K}_V\boldsymbol{V}_a \tag{16}$$

The above equation shows that in order to decouple each degree of freedom, the matrix $\boldsymbol{T}_a\boldsymbol{K}_s\boldsymbol{T}_a^{\mathrm{T}}$ should be diagonal, which is accomplished for $k_{s1}=k_{s3}$ and $k_{s2}=k_{s4}$. In this case, from (8), (9), (11) and under the assumption that the wafer is rigid, we find that all the nominal gap lengths are equal, and from (9) and (13) we obtain that $k_{V1}=-k_{V2}=k_{V3}=-k_{V4}=k_V$, $k_{sj}=k_s$, where $j=1,\ldots,4$. This implies that to decouple each degree of freedom and to simultaneously satisfy the condition for zero wafer potential, all the nominal gap lengths should be equal and all the bias voltages should have the same absolute value. On the basis of the foregoing, if we introduce a new control voltage vector $\boldsymbol{V}=(V_j)^{\mathrm{T}}$, where $j=1,\ldots,4$, which is defined by

$$\boldsymbol{V}=\boldsymbol{T}_e\boldsymbol{V}_a \tag{17}$$

where $\boldsymbol{T}_e=\mathrm{diag}(1\ -1\ 1\ -1)$, the linearized wafer dynamic equation (16) becomes as follows

$$\ddot{\boldsymbol{r}}=k_s\boldsymbol{M}^{-1}\boldsymbol{T}_a\boldsymbol{T}_a^{\mathrm{T}}\boldsymbol{r}+k_V\boldsymbol{M}^{-1}\boldsymbol{T}_a\boldsymbol{V} \tag{18}$$

From (18), we can observe the unstable open-loop wafer dynamics which necessitates the utilization of feedback control for stabilization.

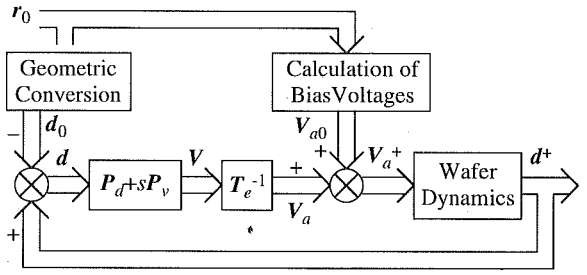

Fig. 3 Block diagram of closed-loop control system.

4. Stabilizing Controller

To implement a stable suspension, a decentralized control scheme, one in which the individual gap lengths at each electrode are controlled independently, is utilized as shown in Fig. 3. Let $\boldsymbol{P}_d$ and $\boldsymbol{P}_v$ be the proportional and derivative gain matrices which are defined by $\boldsymbol{P}_d=\mathrm{diag}(p_{dj})$ and $\boldsymbol{P}_v=\mathrm{diag}(p_{vj})$, where $j=1,\ldots,4$, respectively. Then the control voltage $\boldsymbol{V}$ is determined as

$$\boldsymbol{V}=\boldsymbol{P}_d\boldsymbol{d}+\boldsymbol{P}_v\dot{\boldsymbol{d}} \tag{19}$$

From (15), (18) and (19), we obtain the closed-loop wafer dynamic equation

$$\ddot{\boldsymbol{r}}+k_V\boldsymbol{M}^{-1}\boldsymbol{T}_a\boldsymbol{P}_v\boldsymbol{T}_a^{\mathrm{T}}\dot{\boldsymbol{r}}+(k_V\boldsymbol{M}^{-1}\boldsymbol{T}_a\boldsymbol{P}_d\boldsymbol{T}_a^{\mathrm{T}}-k_s\boldsymbol{M}^{-1}\boldsymbol{T}_a\boldsymbol{T}_a^{\mathrm{T}})\boldsymbol{r}=\boldsymbol{0} \tag{20}$$

In order to decouple each degree of freedom, the matrix $\boldsymbol{T}_a\boldsymbol{P}_d\boldsymbol{T}_a^{\mathrm{T}}$ and $\boldsymbol{T}_a\boldsymbol{P}_v\boldsymbol{T}_a^{\mathrm{T}}$ should be diagonal which is satisfied for $p_{d1}=p_{d3}$, $p_{d2}=p_{d4}$, $p_{v1}=p_{v3}$ and $p_{v2}=p_{v4}$. Let $p_{d2}=\alpha p_{d1}=\alpha p_d$. Then, $\boldsymbol{P}_d$ becomes

$$\boldsymbol{P}_d=p_d\,\mathrm{diag}\,(1\ \alpha\ 1\ \alpha) \tag{21}$$

and $\boldsymbol{T}_a\boldsymbol{P}_d\boldsymbol{T}_a^{\mathrm{T}}$ can be computed as

$$\boldsymbol{T}_a\boldsymbol{P}_d\boldsymbol{T}_a^{\mathrm{T}}=p_d\begin{bmatrix}2+2\alpha & 0 & 0\\ 0 & 2\alpha r_a^2 & 0\\ 0 & 0 & 2r_a^2\end{bmatrix} \tag{22}$$

A similar procedure can be followed for $\boldsymbol{P}_v$ and $\boldsymbol{T}_a\boldsymbol{P}_v\boldsymbol{T}_a^{\mathrm{T}}$. Considering the rotational symmetry of the wafer, it is reasonable to set $\alpha=1$ rendering the θ and ψ movements to exhibit the same dynamics. From (21), it can be seen that for $\alpha=1$, the feedback gains for the four stator electrodes will have the same value. In case $\alpha=1$, the closed-loop wafer dynamics becomes

$$\ddot{\boldsymbol{r}}+2k_Vp_v\begin{bmatrix}\frac{2}{m} & 0 & 0\\ 0 & \frac{r_a^2}{J_r} & 0\\ 0 & 0 & \frac{r_a^2}{J_r}\end{bmatrix}\dot{\boldsymbol{r}}$$
$$+2(k_Vp_d-k_s)\begin{bmatrix}\frac{2}{m} & 0 & 0\\ 0 & \frac{r_a^2}{J_r} & 0\\ 0 & 0 & \frac{r_a^2}{J_r}\end{bmatrix}\boldsymbol{r}=\boldsymbol{0} \tag{23}$$

With a proper choice of p_d and p_v, this system can be stabilized and designed to incorporate desired damping

and stiffness. Note that from (23), it is impossible to perform independent controller designs for the three degrees of freedom.

In order to obtain $\boldsymbol{V}$ from (19), the gap lengths $\boldsymbol{d}$ should be known. In our experimental system, every gap sensor is collocated with the point of application of the force of each electrode, so that the gap sensor signals can be directly used as the gap lengths.

5. Experimental Work and Results

5.1 Experimental System Configuration

Figure 4 shows the schematic diagram of the experimental apparatus. The stator electrodes, shown in Fig. 5, are etched to a 35 μm thick copper layer on a glass epoxy base plate. Each electrode has an area of 73.3 cm^2. The four electrodes together form a ring shape pattern. The outer diameter of the ring is the same as that of the wafer and the inner diameter is 40 mm. The electrode plate is supported and leveled by three upper micrometer positioning screws. The suspended object is an 8-inch silicon wafer with a diameter of 200 mm, a mass of 51.3 g, a thickness of 0.725 mm and a resistivity of 0.1 $\Omega \cdot$m. The wafer is supported by three lower micrometer positioning screws beneath the electrodes in order to set the initial gap lengths. Four optical fiber displacement sensors are positioned at the geometrical centers of the electrodes. The distance from the geometrical centers of the electrodes to the origin is 61 mm.

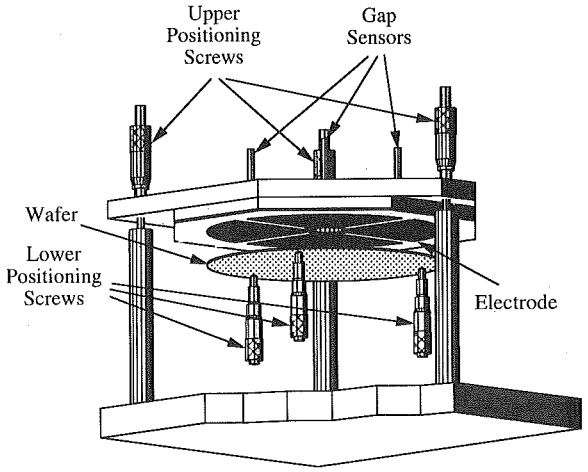

Fig. 4 Schematic diagram of experimental apparatus.

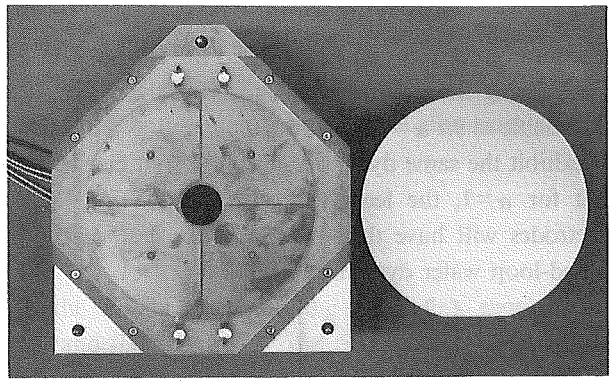

Fig. 5 Photograph of stator and wafer.

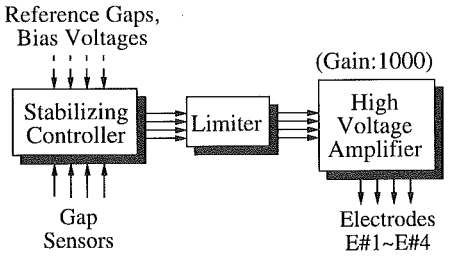

Fig. 6 Structure of control system.

The structure of the control system is shown in Fig. 6. The outputs of four sensors are respectively fed into four controllers as feedback signals. After going through the stabilizing controller, the control voltages are combined with the bias voltages and sent to a limiter circuit which prevents electric discharge. The voltages from the limiter circuit are sent to four dc high-voltage amplifiers and supplied to the four individual electrodes.

5.2 Suspension Experiments

Suspension experiments have been performed in an atmospheric environment. All controller channels have

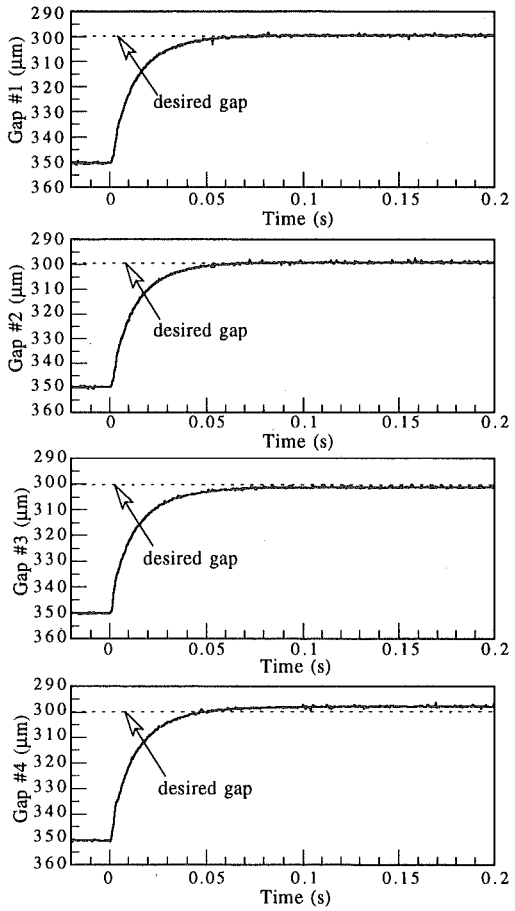

Fig. 7 Gap length variations during suspension process.

the same proportional and derivative gains of which the values are 10^4 kV/m and 25 kVs/m, respectively. A bias voltage of 0.5 kV is supplied to electrodes #1 and #3, and a bias voltage of −0.5 kV to electrodes #2 and #4. A limiter voltage of 1 kV is imposed on electrodes #1 and #3, and a limiter voltage of −1 kV on electrodes #2 and #4. Figure 7 shows the gap length variations after the PD compensators were switched on. It can be observed that from the initial gap length of 350 μm, the wafer was pulled up towards the stator reaching a stable suspension state at a reference gap length of 300 μm in about 70 ms. At the equilibrium position, the gap lengths were 300 μm, 299 μm, 301 μm and 298 μm, respectively. Compared with the reference gap length of 300 μm, the maximum position error was 2 μm. Figure 8 shows the voltage variations during the picking up process. It shows that when the wafer reached the stable suspension position, the voltages applied to the electrodes were 0.5 kV, −0.49 kV, 0.51 kV and −0.48 kV, respectively. Figure 9 shows a photograph which shows the wafer under stable suspension.

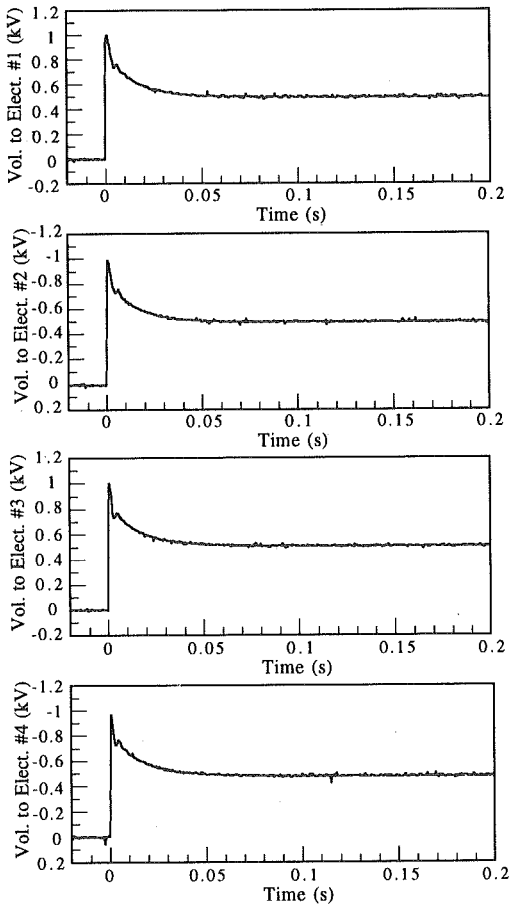

Fig. 8 Voltage variations during suspension process.

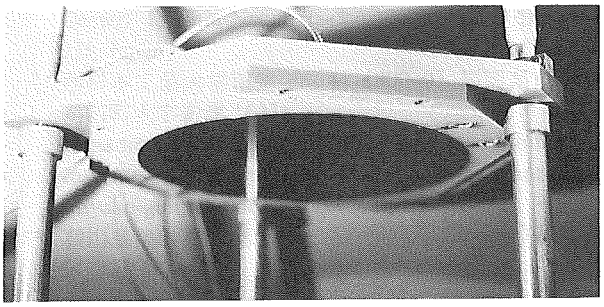

Fig. 9 Photograph showing wafer under stable suspension.

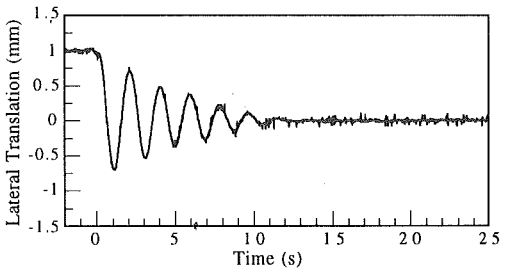

Fig. 10 Dynamic response of lateral motion.

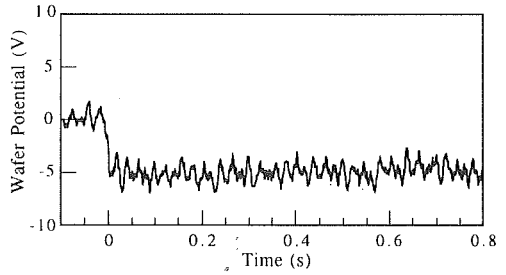

Fig. 11 Wafer potential during suspension process.

5.3 Behavior of Lateral Motion

In the experimental system described above, the lateral motion of the wafer is not actively controlled. However, the experimental results show that the wafer has been levitated horizontally without slipping out in lateral direction. This means that the lateral wafer motion is passively restricted, indicating system stability along lateral direction. Obtaining information on the dynamic behavior along lateral direction may give some insight into the feasibility of electrostatic suspension in all kinds of handling devices. In general the restriction force originates from a relative lateral wafer translation with respect to the stator electrode, causing asymmetry in the stator electrodes-wafer geometry to come into existence, and is a nonlinear function of lateral translation.

The dynamic response of the lateral motion was experimentally explored by using the initial value response method. For small values of lateral translation, the restriction force can be approximated as a linear function of the lateral translation and consequently estimation algorithms for linear systems can be used. The experimental result for an initial lateral translation of 1 mm is shown in Fig. 10. Using the method proposed by Ogata,[11] the estimated values of the damping ratio and natural frequency are about 0.056 and 3.28 rad/s, respec-

tively, while the stiffness is 0.55 N/m. Despite the relatively small stiffness, the wafer can be levitated stably along lateral direction.

5.4 Wafer Potential

The wafer potential variation during the picking up process was measured, as shown in Fig. 11. It shows that at the stable suspension state, the residual potential on the wafer was approximately −5 V. This voltage level neither leads to severe particle adhesion, nor to IC damage on the wafer surface.

6. Conclusions

A contactless silicon wafer suspension system based on electrostatic forces is proposed in this paper. An 8-inch silicon wafer has been suspended successfully at a gap length of 0.3 mm by controlling the electrostatic forces acting on it in an atmospheric environment. The dynamic response of the non-actively controlled lateral motion has also been explored experimentally using the initial value response method and stability along the lateral direction has been confirmed. To prevent wafer potential related IC element damage during suspension, it is crucial to keep the wafer potential close to zero volt. This has been achieved through an asymmetrical electrode potential distribution and was verified through wafer potential measurements during suspension.

The achievement described in this paper reveals that electrostatic suspension has the potential to become an integral part of future contactless and friction-free wafer handling devices for use in high vacuum and clean room environments.

References

1) T. Higuchi, A. Horikoshi and T. Komori: *Proc. 2nd Int. Symp. Magnetic Bearings*, p. 115 (1990)
2) T. Azukizawa and K. Uemura: J. Inst. Electr. Eng. Jpn., **106** (1986) 677
3) M. Ota, S. Andoh and H. Inoue: *Proc. 2nd Int. Symp. Magnetic Bearings*, p. 109 (1990)
4) R.G. Ford and A.S. Koh: *Soc. Manuf. Eng.*, **478** (1990) 1
5) Y. Hashimoto, Y. Koike and S. Ueha: *Proc. 7th Symp. Electromagnetics and Dynamics*, p. 449 (1995)
6) H.W. Knoebel: Control Eng., **11** (1964) 70
7) S.F. Bart, T.A. Lober, R.T. Howe, J.H. Lang and M.F. Schlecht: Sens. Actuators, **14** (1988) 269
8) J. Jin, T. Higuchi and M. Kanemoto: *Proc. 4th Int. Symp. Magnetic Bearings*, p. 343 (1994)
9) J. Jin, T. Higuchi and M. Kanemoto: IEEE Trans. Ind. Electr., **42** (1995) 467
10) M. Tsuji: Proc. Inst. Electrostat. Jpn., **19** (1995) 28
11) K. Ogata: *System Dynamics*, p. 359, Prentice-Hall, New Jersey (1978)

Appendix

Using a linearization technique, we will prove that the wafer potential is zero. Under the conditions (4) and $A_j=A$, where $j=1,\ldots,4$, the wafer potential (6) can be represented as

$$V_f^+=\frac{\sum_{j=1}^{4}\frac{V_{aj}^+}{d_j^+}}{\sum_{j=1}^{4}\frac{1}{d_j^+}} \tag{24}$$

If we linearize the wafer potential around the nominal operating point, then

$$V_f^+=V_{f0}+V_f=V_f=\sum_{j=1}^{4}(k_{vfj}V_{aj}+k_{sfj}d_j) \tag{25}$$

where $k_{vfj}=\frac{\partial V_f^+(V_{a0i},\ d_{0i})}{\partial V_{aj}^+}$, $k_{sfj}=\frac{\partial V_f^+(V_{a0i},\ d_{0i})}{\partial d_j^+}$, $i=1,\ldots,4$

Note that the wafer potential V_{f0} at the equilibrium state is zero as mentioned in (12). By using (15), (17) and (19), and under the following conditions

$$\begin{aligned}&V_{a01}=-V_{a02}=V_{a03}=-V_{a04}\\&d_{0j}=d_0,\ p_{dj}=p_{a0},\ p_{vj}=p_{v0},\ j=1,\ldots,4\end{aligned} \tag{26}$$

we can derive the wafer potential to be zero.

Note that by controlling the electrodes #1 and #3 with negative voltages and electrodes #2 and #4 with positive voltages, the wafer potential can be kept to zero voltage as well. However, when two adjacent electrodes along the circumference, e.g., the electrodes #1 and #2, are supplied with voltages having the same polarity and the remaining two electrodes, e.g., the electrodes # 3 and #4, with voltages having opposite polarity to the polarity of the former two electrodes, the wafer potential will not be zero for wafer positions different from the equilibrium position, even if the wafer potential is zero at the equilibrium position.